NMR Investigation of the Interaction between the Neuronal Protein Tau and the Microtubules†

Alain Sillen,[‡,§] Pascale Barbier,[§,||] Isabelle Landrieu,[‡] Sylvie Lefebvre,[||] Jean-Michel Wieruszeski,[‡] Arnaud Leroy,[‡,⊥] Vincent Peyrot,[||] and Guy Lippens*[,‡]

CNRS UMR 8576 Unité de Glycobiologie Structurale et Fonctionnelle, Université des Sciences et Technologies de Lille 1, 59655, Villeneuve d'Ascq Cedex, France, FRE CNRS 2737 Cytosquelette et Intégration des Signaux du Micro-environnement Tumoral, Faculté de Pharmacie, 27 Bd Jean Moulin, 13385 Marseille Cedex 5, France, and Laboratoire de biochimie appliquée, Faculté de Pharmacie (Paris XI), 5 rue Jean-Baptiste Clément, 92296 Chatenay-Malabry Cedex, France

Received September 15, 2006; Revised Manuscript Received January 5, 2007

ABSTRACT: Whereas the interaction between Tau and the microtubules has been studied in great detail both by macroscopic techniques (cosedimentation, cryo-electron microscopy, and fluorescence spectroscopy) using the full-length protein or by peptide mapping assays, no detailed view at the level of individual amino acids has been presented when using the full-length protein. Here, we present a nuclear magnetic resonance (NMR) study of the interaction between the full-length neuronal protein Tau and paclitaxel-stabilized microtubules (MTs). As signal disappearance in the heteronuclear $^{1}H-^{15}N$ correlation spectra of isotope-labeled Tau in complex with MTs is due to direct association of the corresponding residue with the solid-like MT wall, we can map directly the fragment in interaction with the MT surface, and obtain a molecular picture of the precise interaction zones. The N-terminal region projects from the microtubule surface, and the lack of chemical shift variations when compared with free Tau proves that this region can regulate microtubular separation without adopting a stable conformation. Amino acids in the four microtubule binding repeats (MTBRs) lose all of their intensity, underscoring their immobilization upon binding to the MTs. The same loss of NMR intensity was observed for the proline-rich region starting at Ser214, underscoring its importance in the Tau:MT interaction. Fluorescence resonance energy transfer (FRET) experiments were used to obtain thermodynamic binding parameters, and led to the conclusion that the NMR defined fragment indeed is the major player in the interaction. When the same Ser214 is phosphorylated by the PKA kinase, the Tau:MT interaction strength decreases by 2 orders of magnitude, but the proline-rich region including the phospho-Ser214 does not gain sufficient mobility in the complex to make it observable by NMR spectroscopy. The presence of an intramolecular disulfide bridge, on the contrary, does lead to a partial detachment of the C-terminus of Tau, and decreases significantly the overloading of Tau on the MT surface.

The neuronal protein Tau, as one of the microtubule associated proteins (MAPs[1]), promotes the polymerization of tubulin into microtubules (MTs), and stabilizes the latter (*1*). Whereas electron diffraction has yielded a high-resolution structure of the microtubule and its tubulin heterodimer protein component (*2*, *3*), the details of the molecular interaction between Tau and the tubulin heterodimers or the MT surface, as well as the molecular mechanism of Tau's polymerizing potential, have not yet been elucidated. The natively unstructured nature of Tau when isolated in solution (*4*, *5*) leaves open many possibilities as for its exact structure in the complex with the tubulin surface. The three or four repeating segments found in the C-terminal half of the protein, depending on the isoform under consideration, certainly participate in the interaction, and have received the name of "microtubule binding repeats" (MTBRs) (*1*). However, when considered as isolated subunits, these peptides do not bind strongly to the MTs, but need other parts of the protein such as the proline-rich region to enhance their binding (*6*). Only very recently, the report of a first ordered structure of Tau when complexed to a liposome (*7*) suggests that Tau indeed might adopt a helical conformation within several of its repeats, and hence might interact in a helix−

† A.S. was funded by a European Training and Mobility Grant (HPRN-CT-2002-00241). Part of this work was funded by the Agence National de la Recherche Grant ANR-05-BLANC-0320-01 to G.L. and V.P. The 600 MHz facility used in this study was funded by the Région Nord-Pas de Calais (France), the CNRS, and the Institut Pasteur de Lille. The 800 MHz spectrometer was funded within the French National project "NMR et Radiocristallographie structurale−Grand Bassin Parisien" by the CNRS, Région Nord-Pas de Calais (France), the European Community (FEDER), the French Research Ministry, and the University of Sciences and Technology of Lille I.

* To whom correspondence should be addressed. Tel: (33) 3 20 33 72 41. Fax: (33) 3 20 43 69 49. E-mail: Guy.Lippens@univ-lille1.fr.

‡ Université des Sciences et Technologies de Lille 1.

§ These authors contributed equally to the work.

|| FRE CNRS 2737 Cytosquelette et Intégration des Signaux du Micro-environnement Tumoral, Faculté de Pharmacie.

⊥ Laboratoire de biochimie appliquée, Faculté de Pharmacie (Paris XI).

[1] Abbreviations: AD, Alzheimer's disease; FRET, fluorescence resonance energy transfer; HSQC, heteronuclear single quantum spectroscopy; MAP, microtubule associated protein; MT, microtubule; MTBR, microtubule binding region; NMR, nuclear magnetic resonance; PHF, paired helical filament.

10.1021/bi061920i CCC: $37.00
Published on Web 02/21/2007

helix mode with the C-terminal helices on the α- and β-tubulin proteins. If true, this would be the "internal binding mode" implicating the H11 and H12 helices between the subtilisin and formic acid cleavage sites (*8*). However, despite this novel structural hypothesis, at this date even a precise limit for the complete interacting region in the full-length protein is not known.

Beyond its physiological role of MT interacting protein, Tau is equally involved in the pathology of Alzheimer's disease (AD). Its aggregation into macroscopic paired helical filaments (PHFs) is one of the molecular hallmarks of AD (*9*, *10*). The precise mechanistic factors that detach Tau from the MT surface and lead it to form those fibrillar structures are not known, but oxidative stress, followed potentially by calpain cleavage at its C-terminus to yield a more aggregation prone molecule, is one possible factor (*11*). Another factor influencing directly the interaction of Tau with MTs is its phosphorylation state. Indeed, phosphorylation on several sites has been reported to weaken the Tau:MT interaction and to diminish the polymerizing potential of Tau *in vitro* (*12*−*14*). *In vivo*, this post-translational mechanism, which is tightly regulated by an impressive number of kinases, is involved in the dynamic character of MT polymerization. An additional important impetus to study Tau phosphorylation is that the protein, when integrated in PHFs in diseased neurons, is invariably hyperphosphorylated (*15*).

In this report, we apply NMR spectroscopy to further detail the Tau:tubulin interaction. Using ^{15}N labeling as a filter to distinguish only Tau derived amide groups together with the fact that molecular mobility directly relates to NMR line widths, our experimental setup allows a direct view on those regions of Tau that are in complex with the macroscopic object that is the microtubule, and comparison with fluorescence resonance energy transfer (FRET) results using acrylodan-labeled Tau allows us to resolve the stoichiometry issue of this interaction. NMR spectra on samples with increasing amounts of Tau together with fluorescence and cosedimentation assays were used to probe the possible accumulation of Tau at the MT surface. The influence of different factors such as the oxidation state of the two cysteines of Tau or its post-translational modification by phosphorylation was evaluated by the same experimental approach. Together, these experiments give novel insight into the Tau interaction at the molecular surface of stabilized MTs.

RESULTS

Macroscopic Characterization of the Tau:Microtubule Complex. Polymerization of tubulin into microtubules (MTs) was effected through the addition of paclitaxel and incubation at 37 °C (see Materials and Methods). When centrifuging the resulting sample for 20 min, a SDS−PAGE on the supernatant and resuspended pellet showed that most of the tubulin is in the pellet. When we added a substoichiometric amount of Tau to these microtubules, and again separated supernatant and pellet by centrifugation, we found Tau mostly in the pellet (Figure 1A, lanes 1 and 2), confirming the strong interaction between our Tau preparation and the MTs.

The same strategy was used to further characterize the stoichiometry of Tau binding to MTs, by adding increasing amounts (from 2.5 to 20 μM, Figure 1A) of Tau to the same 5 μM paclitaxel-stabilized MTs, and dosing the amount of soluble Tau in the supernatant and MT bound Tau in the pellet. Based on 3 independent measurements, the resulting Scatchard plots yielded 3.4 ± 0.2 identical binding sites (n) and a site equilibrium dissociation binding constant, k_D = 1.6 ± 0.8 μM (Figure 1B). Importantly, because the SDS−PAGE cannot dose reliably Tau concentrations below 1 μM, one cannot determine whether there exist two binding modes with a high and lower affinity, and even less quantify the binding parameters for both modes (*16*). Electron microscopy confirmed the formation of *bona fide* MTs (Figure 1C). However, despite the apparent accumulation of Tau on the MT surface, the macroscopic aspect of the Tau loaded fibers as revealed by this technique was not significantly different from the initial MTs and did not allow the direct detection of Tau (*17*). Only at the largest excess of Tau used, we observed some bundling of the MTs, in agreement with earlier observations (*18*).

In an elegant study using Tau labeled with acrylodan on its two cysteine residues (Cys291, Cys322), Makrides et al. exploited the energy transfer between tryptophan and tyrosine residues of tubulin as donor to the fluorophore acrylodan as receptor in order to derive thermodynamic binding parameters between Tau and microtubules (*19*). The tubulin−Tau distance hence is comparable to the Förster distance, i.e., typically in the range of 20−60 Å, and FRET provides a powerful and complementary tool to quantify the interaction between microtubule and Tau. First, we performed the experiment with our Tau sample marked with acrylodan on both cysteines, and obtained values for the dissociation constant k_D = 20 ± 4 nM and for the number of Tau binding sites per tubulin dimer n = 0.40 ± 0.04 (Figure 2), in good agreement with the previously reported values. The discrepancy with the cosedimentation results therefore suggests that FRET only observes the direct Tau:MT interaction, whereas the cosedimentation assay detects all bound Tau protein, be it directly to the microtubules but far away from its aromatics or via a putative Tau−Tau interaction (*20*).

HETERONUCLEAR NMR SPECTRA OF TAU BOUND TO MICROTUBULES

A first sample with microtubules at a final concentration of 100 μM tubulin gave no workable results (data not shown). Indeed, even the deuterium lock signal proved difficult to detect. At these concentrations, the microtubules form a partially aligned liquid crystalline phase that can couple strongly with the water protons through the large amount of exchangeable hydroxyl protons on the tubulin poly-glutamate peptides. Using birefringence, Hitt et al. had found that, below a limiting concentration of 38 μM tubulin, the MTs do not form this phase anymore (*21*). The signal deterioration observed in a recent NMR study (*22*), where the Tau:MT interaction was probed by increasing the MT concentration and hence reached beyond this limit, might come from this partial orientation of the MTs rather than from a phenomenon related to the Tau:MT interaction. This result prompted us to repeat the study with a starting concentration of 20 μM paclitaxel-stabilized microtubules (where we give the concentration of tubulin heterodimers), to which 5 μM ^{15}N-labeled Tau was added. This latter value leads to a Tau:tubulin ratio below the FRET derived stoichiometry, while simultaneously giving enough protein to be detectable at 600

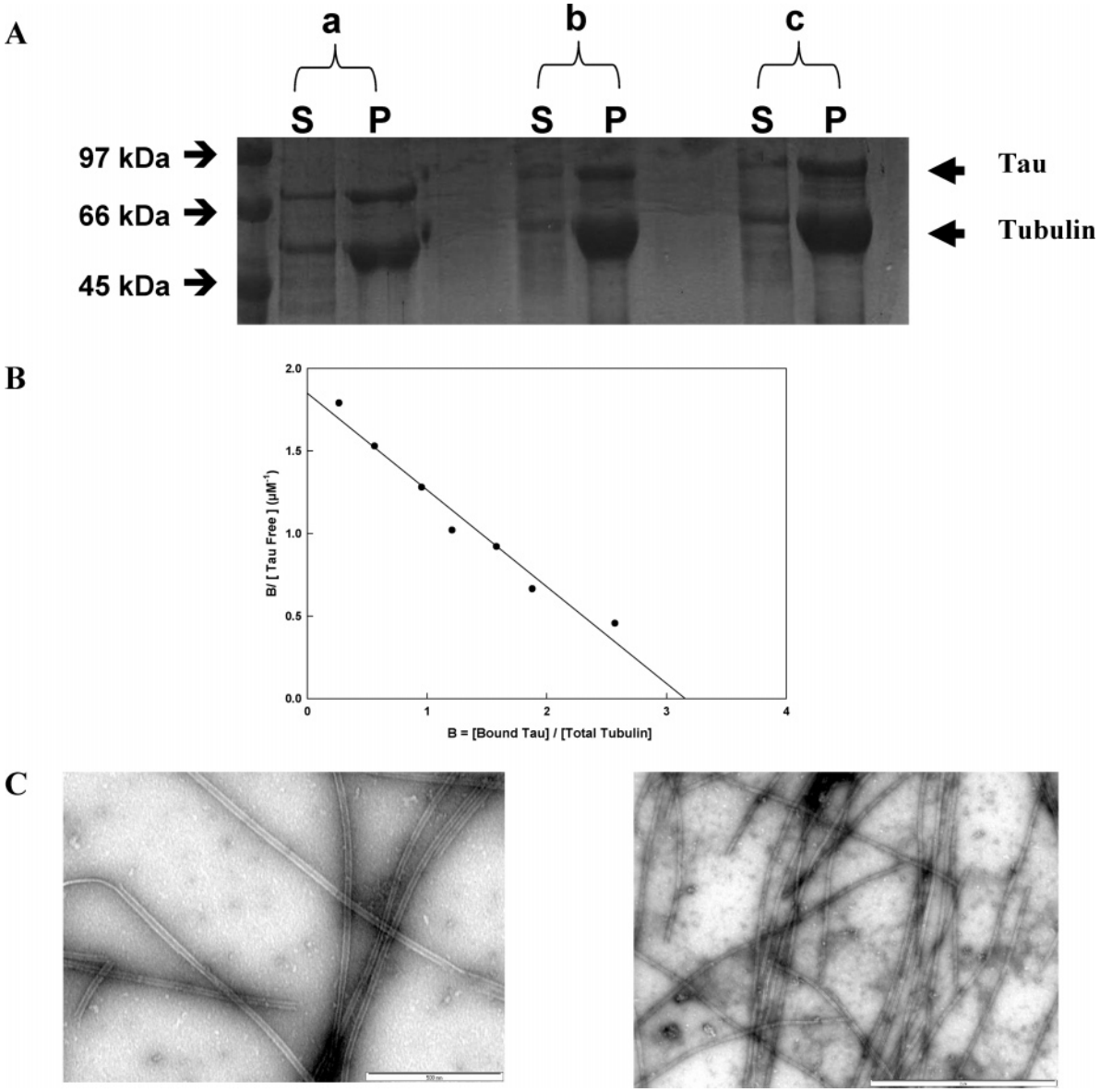

FIGURE 1: (A) SDS−PAGE analysis of the Tau−microtubule interaction. A fixed concentration of tubulin (5 μM) was mixed with different Tau concentration and centrifuged (see Materials and Methods), and the pellet (P) and the supernatant (S) were collected and analyzed on the gel. Tau concentrations are 5 μM (a, lanes 1 and 2), 8 μM (b, lanes 3 and 4), and 10 μM (c, lanes 5 and 6). (B) Scatchard plot of the binding of Tau on paclitaxel-stabilized microtubules in the presence of 0.4 mM DTT. Binding parameters for this particular experiment derived are $k_D = 1.7$ μM and $n = 3.2$. (C) Electron microscopy of MTs with Tau bound in substoichiometric conditions (0.5:1, left), and in a large excess (10:1, right). The bar represents 500 nm.

MHz with a cryogenic probe head in an overnight experiment. When trying to run spectra with less Tau but over a longer time span, we invariably observed degradation and/or precipitation of the NMR samples, consistent with the limited stability of microtubules.

Comparing the spectra of free Tau with that of Tau in complex with the paclitaxel-stabilized MTs (Figure 3), we observed the disappearance of a large body of the resonances. The nanomolar affinities derived from the FRET experiments exclude that signal disappearance is due to chemical exchange broadening, and point to the immobilization in a high molecular weight complex as the main culprit. Our partial assignment of the Tau HSQC spectra (*23*, *24*) together with the assignments of the K18 and K19 fragments (*22*, *25*) was used to map precisely the signal intensity on the primary sequence of Tau (Figure 3). The N-terminal projection domain only partially maintains its full intensity (as defined by a sample of the same concentration of freely soluble Tau), with a relative intensity ratio >90% for all residues up to Ile108 followed by a roughly linear decrease of intensity up to Ser214, which is the first residue whose intensity in the bound state is below 20% of its unbound intensity. Signals of all assigned peaks between Val226 and Glu372 invariably are below this threshold, thereby confirming that residues in all four repeat regions do strongly bind to the MT surface and hence lose their residual mobility and NMR signal. The first assigned residue that again overcomes this value is Thr377, and intensity slowly further increases for the C-terminal residues up to the final Leu441, where the correlation peak of this latter residue is characterized by a relative intensity of 50%. In order to determine whether the region of disappearing intensity provided the essential contacts determining the interaction strength, we overexpressed and purified two fragments of Tau, Tau-[207−421]

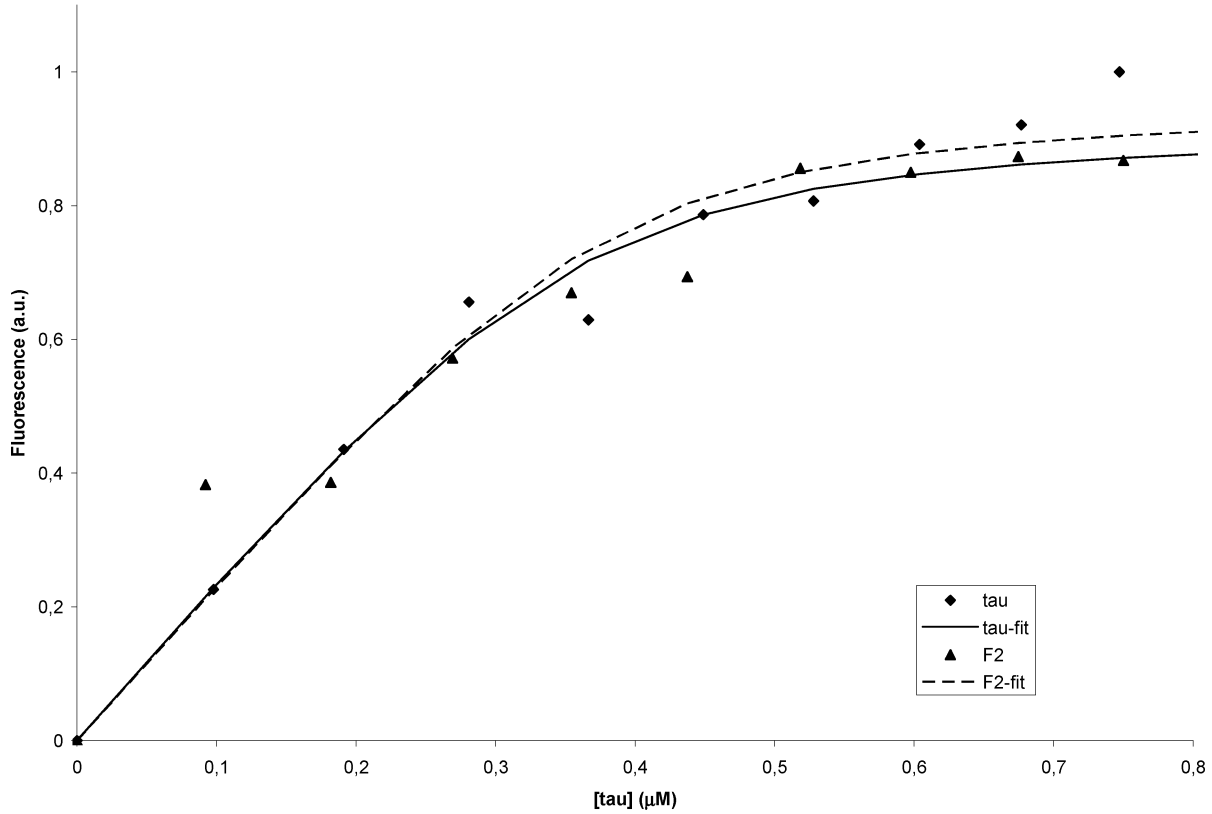

FIGURE 2: FRET measurement of the binding parameters of acrylodan-labeled full-length Tau-[1−441] (diamonds, solid line) or of the fragment Tau-[Ser207−Ser421] (triangles, dotted line) to paclitaxel-stabilized MTs. The titration was done against a fixed (1 μM) concentration of MTs. Plotted is the normalized fluorescence intensity measured at 480 nm.

and Tau-[163−441], that we previously had used to help in the NMR assignment (*24*), and that contain both the proline-rich region and the 4 MTBRs. The NMR spectrum of these fragments bound to the MT surface contained only a few peaks from the terminal residues, confirming that they indeed span the MT binding region (Figure S1, Supporting Information). More importantly, when we labeled the Tau-[207−421] fragment with acrylodan, and performed the same FRET assay as for full-length Tau, we found a very similar value for the dissociation constant ($k_D = 26$ nM), and no significant change in the stoichiometry ($n = 0.39$) (Figure 2, dotted line). This indicates that the Tau fragment that completely loses its mobility upon interaction with the MTs is the main contributor to the binding strength, whereas the other parts do not contribute significantly.

We further recorded spectra of additional samples with increasing Tau:MT ratios. The overall aspect of the spectrum with a 1:1 ratio was the same as in Figure 3, with relative intensities within 10% of the ones determined for the initial 1:4 sample. In an effort to saturate the microtubule surface, we prepared a new sample of 5 μM paclitaxel-stabilized microtubules and added an excess of ^{15}N-labeled Tau. Cross-peak intensities of those residues whose presence at the interaction surface was inferred from their NMR signal disappearance in the substoichiometric samples did not reappear even at a ratio of 3:1 (Figure 4). Because Tau in our conditions is very soluble, we recorded a sample with a 10-fold excess (50 μM), and did observe this time all resonances, be it with a reduced intensity for the interacting residues. Because NMR signals will disappear when the nuclei involved have lost their mobility, irrespective of the nature of the interaction (direct or indirect), this observation is in agreement with the initial cosedimentation experiment, and we conclude that Tau can accumulate onto the surface of the microtubules, as was previously proposed (*20*).

Influence of the Oxidation State of Tau. Although the extent of microtubule polymerization changes only slightly for samples containing oxidant-treated Tau with the disulfide bridge formed between both cysteines (*26*), we wondered whether the presence of an intramolecular disulfide bridge would interfere with Tau binding to the microtubules. In the absence of DTT, Tau in a concentration range from 0.031 to 0.5 mg/mL when loaded on the SDS−PAGE displays a major band just above the migration position of the albumin marker at 67 kDa and two minor bands above the migration position of phosphorylase b at 94 kDa (Figure 5, left), where the latter two weak bands probably correspond to low oligomeric forms (dimer and trimer) linked by a disulfide bridge. In the presence of DTT, Tau in the same concentration range displays only one band that migrates just at the position of the albumin marker at 67 kDa (Figure 5, left). Under our NMR conditions, we conclude from this that Tau is mainly monomeric. As no free sulfhydryl groups could be detected by reaction with 5,5′-dithiobis(2-nitrobenzoic acid) (DTNB), we moreover conclude that the major fraction contains the intramolecular disulfide bridge. The chemical shift variations for residues near the cysteines confirm this finding, as we note mainly chemical shift variations for residues in the loop between both Cys291 and Cys322, but not outside this loop (Figure 5).

The FRET assay being impossible because acrylodan labeling is done via the cysteines, we repeated the previous NMR binding experiment without DTT. The spectrum with a substoichiometric amount of Tau (0.25:1 Tau:tubulin)

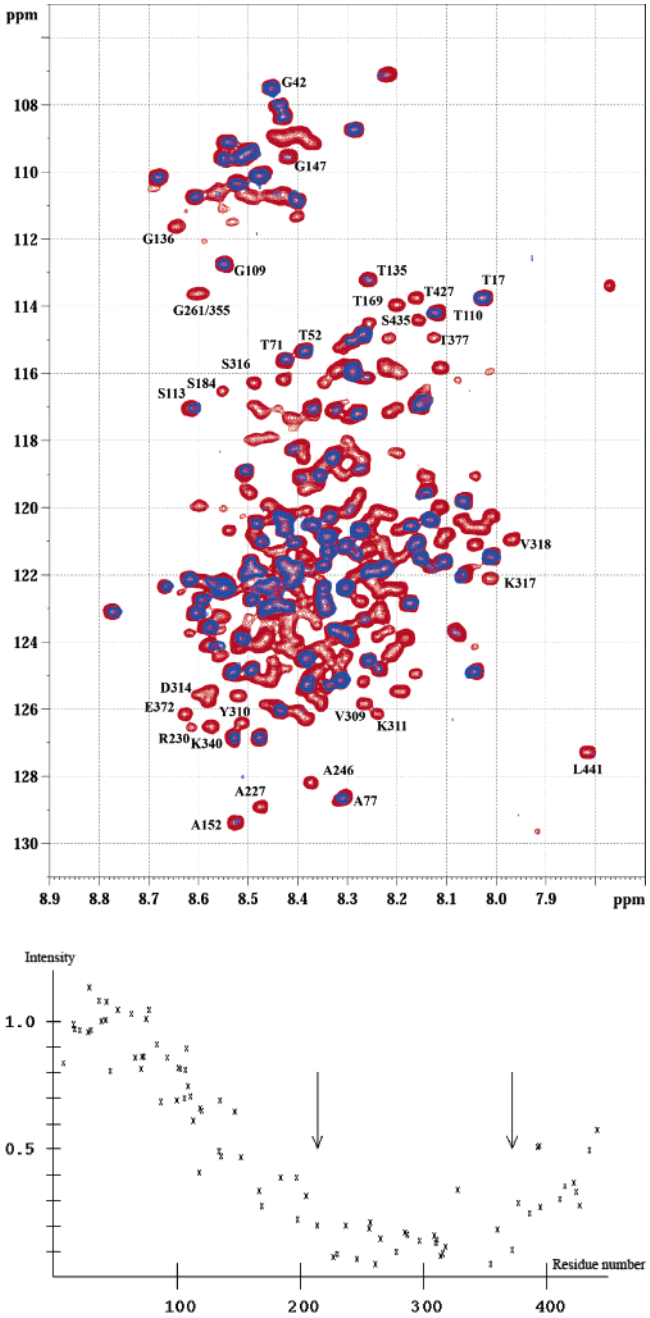

FIGURE 3: (top) $^{1}H-^{15}N$ HSQC spectrum of free Tau (red) and of Tau in the 0.25:1 complex with paclitaxel-stabilized MTs (blue). (bottom) Relative intensities of the amide resonances as a function of sequence number. Arrows indicate residues 214 and 372, that span the zone of residual intensity <20%.

showed significantly more intensity than its counterpart in the presence of DTT, indicating a lesser immobilization of Tau on the MT surface in these oxidizing conditions. Whereas the effect is already pronounced in the N-terminal projection domain, where without DTT the threshold of 90% is maintained for residues up to Thr135 and the signal ratio does not decrease below 20% before Met250 (Figure S2, Supporting Information), the effect of the intramolecular disulfide bridge is even more pronounced at the C-terminus of the protein (Figure 6). The first residue that reaches an intensity ratio superior to 70% is Thr403, and we obtain 95% for the C-terminal Leu441. Therefore, the oxidation state of the disulfide bridge in Tau alters its binding to the microtubule surface and seems to lessen the interaction at its extremities. When we repeated the cosedimentation assay as a second macroscopic method to evaluate the interaction in the absence of DTT, we found $k_D = 0.4 \pm 0.3$ μM, with $n = 1.0 \pm 0.4$. We confirmed this lesser saturation of Tau on the MT surface when the intramolecular loop is formed by NMR, as even with a slight excess of Tau, signal intensity reappeared for the same downfield shifted Ala residues that in the presence of DTT did not recover intensity before a 3-fold excess (Figure 4).

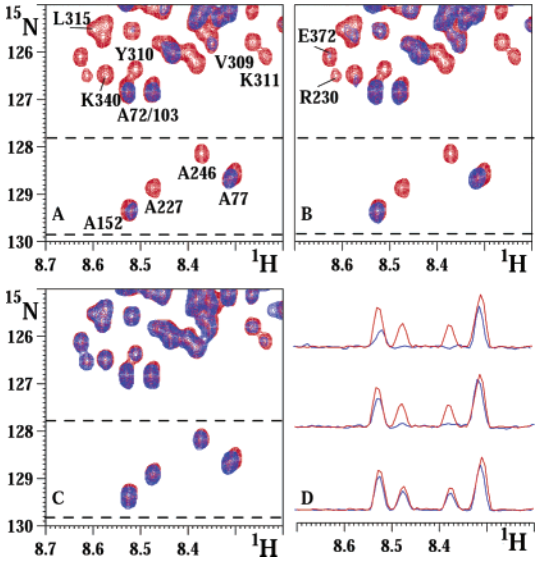

FIGURE 4: Spectra of Tau:MT samples with a stoichiometry of 1:1 (top, left), 3:1 (top, right), and 10:1 (bottom, left), and partial projections between the dotted lines (bottom, right). Projections correspond to the region of the 3 HSQC spectra with ^{15}N frequencies between 128 and 130 ppm. The resulting 1D proton spectra for the 1:1, 3:1, and 10:1 samples are shown from top to bottom.

Influence of the Phosphorylation of Tau. Phosphorylation at the Ser214 site has been reported to decrease the interaction between Tau and the MTs (*27*). We produced a PKA phosphorylated ^{15}N-labeled Tau sample, and exploited the fact that phosphorylation downfield shifts the NMR frequency of the amide proton by almost 1 ppm. As such, we could verify that phosphate integration in the Ser214 side chain was the first one to be effected by the PKA enzyme, was completed for more than 85% of the sample, and was moreover unique, as no other amide proton signal appeared around 9 ppm when using short incubation times (*28*). We thus acrylodan-labeled this pSer214-Tau, and performed the same FRET binding assay with the non-phosphorylated Tau. Fitting the curve led to values for $k_D = 2.3$ μM and $n = 0.4$ (Figure 7), indicating that this unique phosphorylation event can reduce the affinity 100-fold. Because this same Ser-214 residue was one of the first ones for which the amide signal disappeared in the Tau:MT complex (Figure 3), we added the ^{15}N-labeled pSer214-Tau in the same 0.25:1 stoichiometry as above to the paclitaxel-stabilized microtubules. As before, the MTBR residues again lost most of their intensity, confirming that with the kDa value derived and given the initial conditions of 5 μM Tau and 20 μM tubulin, 90% of Tau still should be bound to the MT surface. More importantly, not only did we find very little change in the reduced intensity profile that was observed for unmodified Tau (Figure 3) but, in particular, the pSer214 signal

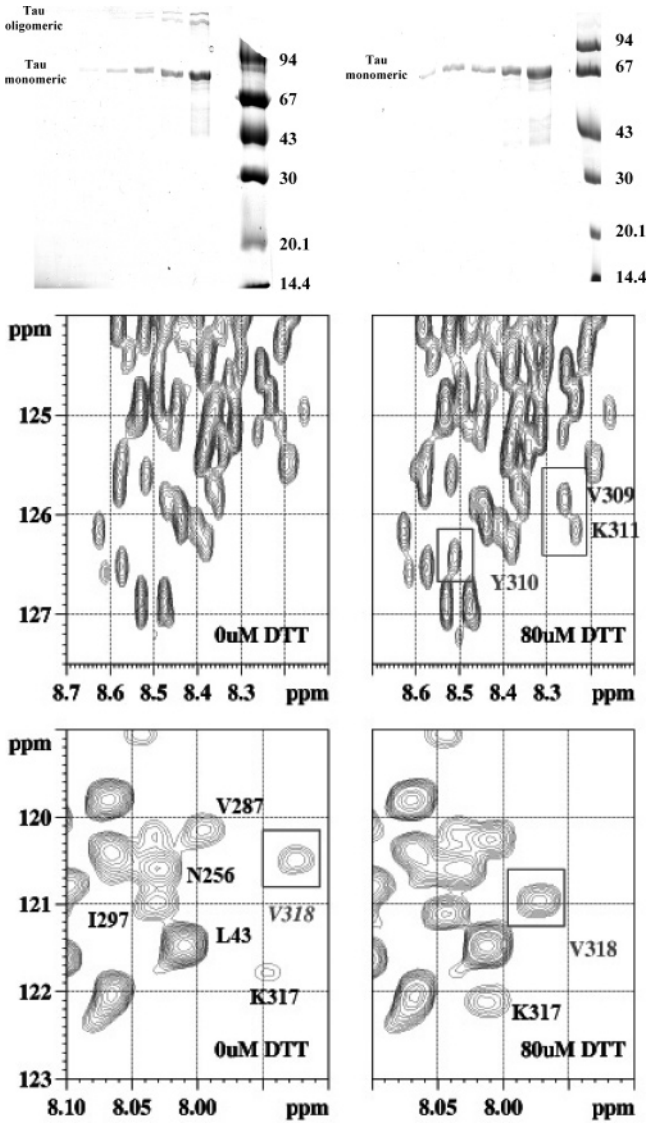

FIGURE 5: (top) SDS−PAGE of Tau in the absence (left) or presence (right) of DTT. In both cases, the monomeric form is the dominant species. (bottom) HSQC spectra of native Tau in the absence (left) or presence (right) of DTT, showing that the resonances of residues between both cysteines specifically shift.

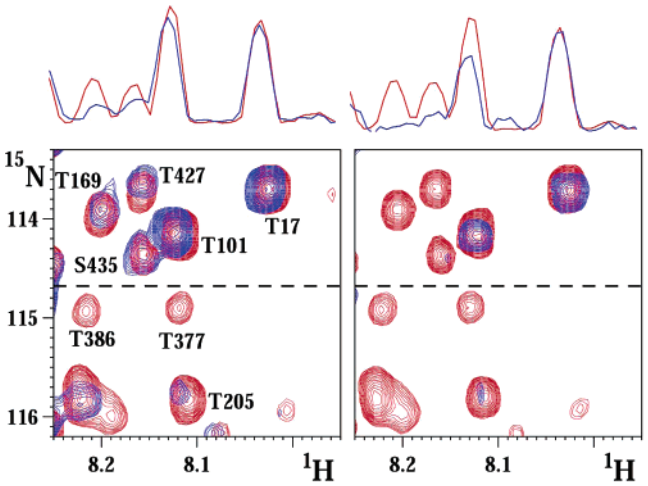

FIGURE 6: Comparable spectra of 5 μM Tau bound to 20 μM paclitaxel-stabilized MTs in the absence (left) or presence (right) of DTT. The partial projections are constructed from the upper half of both spectra.

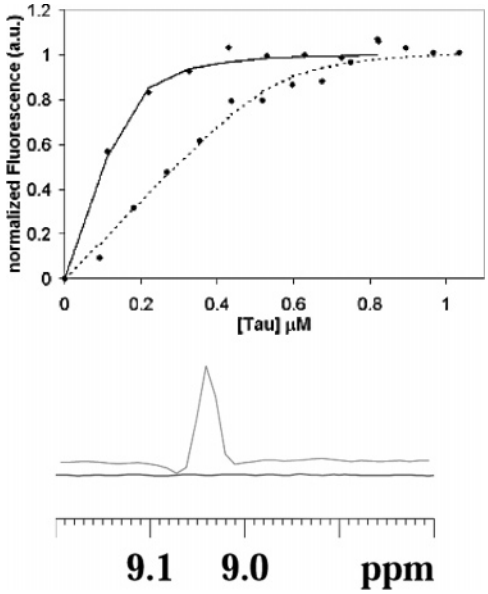

FIGURE 7: (top) FRET measurement of the binding parameters of acrylodan-labeled full-length Tau (diamonds, solid line) or of the pSer214 Tau (spheres, dotted line) to paclitaxel-stabilized MTs. Titration was done against a fixed (1 μM) concentration of MTs. (bottom) Cross section through the amide correlation of pSer214 for phospho-Tau free in solution (red) or phospho-Tau bound to the MTs (black).

completely disappears, demonstrating that although the modification reduces the interaction strength 100-fold, the residue does not dissociate from the surface and gain sufficient mobility to be observable in a liquid-state NMR experiment (Figure 7).

DISCUSSION

Cosedimentation of the microtubule surface immobilized Tau molecules, while keeping the Tau or tubulin concentrations constant (*16*, *20*, *29*) as well as fluorescence FRET spectroscopy with acrylodan-labeled protein (*19*) have been used to probe in detail the thermodynamic and kinetic binding parameters of the Tau:microtubule complex. We have repeated here several of these experiments, and confirm the substoichiometric binding as determined by the fluorescence assay using the acrylodan-labeled Tau. However, we can get overloading of the surface, as shown by our cosedimentation assay where we can load up to 3 Tau molecules per tubulin dimer. Peptide mapping studies have allowed characterization of the interaction as a network of weakly interacting sites (*29*), with a more specific role for the R1−R2 inter-repeat region (*6*, *41*), but no detailed view of the interacting region has been obtained when using the full-length protein.

Early attempts to apply NMR spectroscopy to the characterization of microtubule associated proteins had concluded from the appearance of novel signals upon adding the MAP to microtubules that at least part of these proteins maintained a certain degree of flexibility in the molecular complex (*30*). Here, we have extended this observation by using ^{15}N-labeled Tau, and applying heteronuclear NMR spectroscopy to its complex with paclitaxel-stabilized MTs. Several technical concerns determined the experimental conditions: we consistently wanted to remain below the critical concentration where the microtubules can form a liquid crystalline phase

(*21*). Our present effort to map the primary Tau:tubulin interaction by NMR spectroscopy requires avoidance of the stacking problem, early on recognized as a potential problem in the characterization of the Tau:microtubule complex (*29*). A Tau:tubulin ratio below the maximal number of Tau binding sites per tubulin dimer should circumvent this problem, as the overloading is significantly weaker than the primary Tau:tubulin interaction (*29*). This first condition, together with the technical feasibility to obtain a satisfactory signal-to-noise ratio on a time scale where the sample would not degrade during the NMR experiment, prompted us to work with a 20 μM polymerized tubulin and 5 μM ^{15}N-labeled Tau. This 1:4 Tau:MT ratio is below the 1:2 ratio determined by separating free and bound Tau added onto a fixed concentration of paclitaxel-stabilized microtubules (*20*), or the 1:3 stoichiometry as determined recently by a FRET assay (*19*), and should therefore give us a per-residue view on the true interaction between Tau and the microtubule surface. Moreover, with the sub-micromolar dissociation constant as determined by FRET (our study and ref *19*), the complex is stable on the NMR time scale, and we expect no broadening of signals due to intermediate exchange. The complex becomes very large, however, and because we used neither deuteration nor relaxation optimized pulse sequences (*31*), amide functions of amino acids immobilized at the surface of the MT are expected to lose most if not all of their intensity in the NMR spectrum.

Whereas the N terminus of Tau was shown to influence the in vivo spacing between micotubules (*32*, *33*) and even to disperse densely packed bundles of microtubules (*34*), how it performs this task is still unknown. As the chemical shift is an exquisitely sensitive probe for the local environment of a given nucleus and molecular flexibility determines the line width of the NMR signal, the peak position and residual intensity of an individual correlation peak in the resulting HSQC spectrum are good probes for the structure and dynamics of the individual amino acid. The perfect superposition of the NMR signals of free and MT bound Tau within the first 100 amino acids (Figure 3), including the two N-terminal inserts that distinguish the longest adult from the shortest fetal isoform, prove that this N-terminal stretch retains the dynamic character it adopts in the free protein, and does not require a stable structure to separate the microtubules.

For the next 100 residues, the chemical shift equally is identical to that of the corresponding amide functions in the free Tau, but their intensity gradually decreases to vanishing levels, with Ser214 being the first residue with its residual intensity below 20%. Despite the power of NMR spectroscopy to probe the dynamics at different time scales of amide functions in a protein, different attempts to do so in the present sample were unsuccessful. Indeed, the low concentration of ^{15}N-labeled Tau (5 μM) together with the limited stability of the MTs under the NMR conditions (with consistent sample degradation after one night scanning at 20 °C) excludes heteronuclear relaxation measurements. However, we have previously described a similar NMR behavior for the N-terminal part of Tau (running up to Gly261) that was not incorporated in the rigid core of heparin-assembled Tau paired helical filaments (*35*). In this latter context, sample concentration and stability were not as critical, making a heteronuclear relaxation study feasible. Our conclusion that the marginal reduction of local correlation time τ_c could not explain the intensity drop (*35*) is probably valid here as well. We currently favor the hypothesis that the intensity drop stems from the rapid but not fully isotropic movements for those residues in close vicinity to the MT wall. Besides the rigid character of the MT wall, the heterogeneous nature of the polyglutamate peptides that constitute the C-terminus of both α- and β-tubulin (*36*) can equally contribute to this anisotropy. The amide protons and nitrogens of residues in the vicinity of the MT surface will therefore experience a slightly different chemical shift according to the orientation of the macroscopic MT (or PHF) axis with respect to the magnetic field. As the MTs (or PHFs) do rotate isotropically at the subcritical concentrations used, we recover the isotropic chemical shift identical to that in the isolated Tau molecule, but the averaging occurs on the slow time scale of the macroscopic MT rotational diffusion and hence leads to a line broadening. The degree of anisotropy depending directly on the distance of the residue from the MT wall, we obtain the linear intensity gradient. It should be noted that, although the charge neutralization of this acidic region near the carboxyl-terminal of tubulin by basic compounds may be necessary for tubulin polymerization (*37*, *38*), the lack of chemical shift changes suggests that these peptides do not significantly interact with basic residues in the N-terminal projection domain.

Not surprisingly, amino acids in the region from Ser214 to Thr377 lose most of their intensity. This region spans the four MTBRs, identified early on as binding units to microtubules (*39*, *40*) as well as the R1−R2 inter-repeat region with the critical lysines at positions 274 and 281 (*41*). The region of interaction equally spans the proline-rich stretch preceding these MTBRs as well as 10 amino acids downstream of the repeats. Both binding studies with deletion mutants (*16*) and peptide studies (*6*) had determined the essential role of these flanking regions for tight binding to the MTs, with a particularly important role for the K_{224}-$KVAVVR_{230}$ peptide (*6*). The fact that, in our experiments, the region of disappearing intensity starts at Ser214 might indicate that signal disappearance for the first 10 residues is due to dynamical restriction near the surface rather than a direct interaction. Further confirmation on the importance of the proline-rich region came from a recent NMR study of the isolated three or four repeat domains devoid of this domain (*22*), where only line broadening but no signal disappearance was observed upon addition of the Tau constructs to the MTs. In the latter study, though, Tau constructs were systematically in excess of tubulin dimer, suggesting that these NMR results probed the accumulation of Tau at the MT surface rather than the direct Tau:MT interaction.

The proline-rich region contains many of the putative phosphorylation sites of Tau that led both to its detachment of the MTs and to their aggregation into paired helical filaments. However, our information is presently limited to the identification of certain sites that, when phosphorylated, interfere with Tau's role in microtubule assembly and/or with microtubule binding. We have used here a sample phosphorylated for 15 min by the PKA enzyme, where only the Ser214 site is phosphorylated to a large extent (*28*). This pSer214-Tau is strongly reduced in its capacity to assemble tubulin into microtubules (*41*, *42*), and our fluorescence data

indicate that phosphorylation at the Ser214 position reduces 100-fold the binding strength between Tau and the paclitaxel-stabilized microtubules. Nevertheless, the addition of the phosphate moiety does not detach the proline stretch from the surface to such an extent that it becomes observable by NMR spectroscopy. In fact, whereas its amide resonance was the first to fall below the 20% residual intensity threshold we used to define the interaction zone in unmodified Tau, its intensity here remains close to zero (Figure 7), pointing to a complete immobilization. Phosphorylation at the 214 position might therefore have this residue compete for the basic charges of the cluster comprising two lysine residues (Lys224, Lys225) and one Argine at position 230, previously shown to be important for the binding (*6*). This interaction with other residues of Tau (rather than of tubulin) would still immobilize the phosphorylated side chain and prevent its observation by NMR spectroscopy, and might simultaneously explain the important affinity drop that we observed.

The oxidation state of the intramolecular disulfide bridge that can form between cysteines 291 and 322 is expected to change the protein conformation within this region spanning R2 and R3, and might as such influence the interaction beween both macromolecules. The pathological formation of PHFs from Tau is indeed influenced by the oxidation state (*44*), although in the latter study, the formation of the inter- rather than intramolecular disulfide bridge was identified as the PHF promoting factor. The good agreement between SDS−PAGE with or without DTT shows that our Tau sample mainly contains a monomeric fraction with an intramolecular disulfide bridge (Figure 6), and the NMR spectra in the absence or presence of a reducing agent are identical except for those residues between the cysteines (Figure 6). The same NMR experiment hence was performed in the absence of DTT, in order to evaluate whether this loop formed between both cysteines would influence the interaction surface between Tau and the microtubule. Although structural differences in the region of disappearing intensity are undetectable in this experiment, signal intensity was significantly higher at the same substoichiometric ratio of 1:4 Tau:MT but in the absence of DTT (Figure 6). The effect being the most pronounced for the C-terminal peptide spanning the last 40 residues of Tau, this suggests that the region downstream of the fourth repeat loses to some extent its interaction with the MT surface, showing clearly that the different repeats do not interact as independent binding units, but do couple to one another. Two consequences of biological importance of this C-terminal detachment might be an altered bundling of the microtubules according to the oxidation state of the cysteine bridge, but equally a differential accessibility to potential proteases. Indeed, the last 14 amino acids were shown to be directly involved in microtubule bundling, through a coiled hydrophobic zipper model (*45*). Although unclear how this C-terminus will act when simultaneously the N-terminal domain exerts its spacing role, its accessibility upon formation of the intracellular disulfide bridge hence might regulate further the bundling properties of the microtubules, important for the supramolecular structure and correct functioning in the neuronal axon. Second, caspase cleavage at the position Asp421, recently described as an early event in Alzheimer disease tangle pathology (*11*), might be easier when this fragment is detached from the MT surface. Our direct observation that oxidation of the cysteine bridge diminishes the interaction between this peptide and the MT surface hence suggests an additional link between oxidative stress and formation of intraneuronal tangles as observed in Alzheimer's disease.

Cryo-electron microscopy has suggested that Tau binds longitudinally along the outer ridges of paclitaxel-stabilized MT protofilaments (*46*). The FRET derived stoichiometry of 1 Tau per 2 dimers, together with the NMR observation that all 4 MTBRs become immobilized on the surface of the paclitaxel-stabilized MTs, is in agreement with a model where one MTBR would bind per tubulin subunit on an external site. However, both FRET (*19*) and cryo-electron microscopy (*47*) in studies that used Tau rather than paclitaxel as the tubulin polymerizing agent indicated a different irreversible binding site, and even hinted to the possibility that Tau would bind inside the as such formed MTs. Therefore, a detailed picture of the precise interactions between Tau and tubulin residues is clearly awaited to shed light on the precise nature of the interaction. Can NMR spectroscopy lead to information on the interacting fragment of Tau and its conformation in the complex with tubulin? Invisible on our spectra, because of the high molecular weight of the microtubules, labeling with deuterium of the Tau molecule and complex formation with smaller stable constructs of tubulin might indeed offer some hope to obtain molecular details of the interaction surface. Ring structures containing no more than ten tubulin dimers can be formed at 20 °C, leading to complexes in the order of 1 M Dalton (*48*). Whereas a full structure elucidation on such a complex is presently still out of reach, TROSY NMR spectroscopy on complexes of comparable weight (*49*) has given valuable molecular information, and is presently under study in our laboratory.

MATERIALS AND METHODS

Tubulin Purification. Tubulin was purified from lamb brains by ammonium sulfate fractionation and ion-exchange chromatography. The protein was stored in liquid nitrogen and prepared as described previously (*50*). Protein concentrations were determined spectrophotometrically with a Perkin-Elmer spectrophotometer Lambda 800 and an extinction coefficient at 275 nm of 1.07 $L \cdot g^{-1} \cdot cm^{-1}$ in 0.5% SDS in neutral aqueous buffer or 1.09 $L \cdot g^{-1} \cdot cm^{-1}$ in 6 M guanidine hydrochloride.

Tau Purification. ^{15}N-labeled Tau was prepared as described previously (*23*, *24*) and was dosed by absorption. Tau-[207−421] and Tau-[163−441] are fragments generated by PCR amplification of the corresponding cDNA coding sequence from the Tau cDNA, cloned in the pET15b vector (Novagen) in the same manner as the cDNA for Tau441. The phosphorylated Tau sample was prepared by incubating 10 μM ^{15}N-labeled Tau for 15 min with 0.1 μM PKA catalytic domain, as described (*28*).

Paclitaxel-Stabilized Microtubules. Tubulin assembly was performed in phosphate buffer 25 mM, NaCl 25 mM, pH 7, 8 mM $MgCl_2$, DTT 0.4 mM, GTP 0.1 mM. 15 μM tubulin was incubated with 15 μM paclitaxel at 37 °C to induce microtubule formation. The stabilized microtubule solutions were then diluted at desired concentration and titrated with different concentrations of Tau to measure the interaction by NMR or by cosedimentation assay.

Cosedimentation Assay and SDS−PAGE Analysis. 5 μM paclitaxel-stabilized microtubules was titrated by Tau (from 2.5 to 20 μM) at 20 °C. Samples were then centrifuged using a TL-100 Beckman ultracentrifuge with a TLA 100.2 rotor during 20 min at 50000 rpm (88000*g*) at 20 °C to pellet microtubules. We used a cushion of glycerol (*29*) during the centrifugation step to eliminate nonspecific binding. The concentrations of Tau in the pellets (bound Tau) and the supernatants (free Tau) were determined by densitometry on SDS−PAGE with tubulin concentration as standard using Scion Image program available on the Web (http://www.scioncorp.com/frames/fr_scion_products.htm). The binding parameters of Tau on paclitaxel-stabilized microtubules were determined using the graphical representation of Scatchard (B/L vs L, where B = moles bound ligand/moles total receptor and L is the free ligand concentration). Experiments were done in triplicate. Polyacrylamide gel electrophoresis in denaturing conditions (SDS−PAGE) was performed using 12% acrylamide in the separating gel and Amersham Pharmacia low-weight calibration kit (97, 66, 45, 30, 20.1, and 14.4 kDa) for standards. Gels were stained with Coomassie brilliant Blue. Furthermore, using the Ellman's test (*51*) with 5,5′-dithiobis(2-nitrobenzoic acid) (DTNB) we did not observe by spectroscopy the formation of 2-nitro-5 thiobenzoate (TNB) at 412 nm. Therefore we can conclude to the formation of an intramolecular S−S bond between the two cysteine residues present in Tau.

In order to verify the monomeric character of Tau in the presence and absence of DTT, a classical 12% acrylamide gel was prepared using riboflavine and UV light instead of ammonium persulfate for the polymerization of the mixture of acrylamide bisacrylamide in the presence of TEMED, leading to a more reproducible gel. Low molecular weight protein standards from Amersham Pharmacia were used as migration markers in the absence or presence of 1 mM DTT.

Electron Microscopy. Samples were adsorbed onto 200 mesh, Formvar carbon-coated copper grids, stained with 1.5% (w/v) uranyl acetate, and blotted to dryness. Grids were observed using a JEOL JEM-1220 transmission electron microscope operated at 80 kV.

NMR Spectroscopy. $^{1}H-^{15}N$ HSQC spectra were recorded on a 600 or 800 MHz Bruker instrument, where the former was equipped with a cryogenic triple resonance probe head and the latter with a standard triple resonance probe. Spectra on the 5 μM ^{15}N-labeled Tau in the presence of 20 μM paclitaxel-stabilized microtubules with or without DTT were recorded at 20 °C with 128 scans per increment and 128 respectively 1024 complex points in the ^{15}N and ^{1}H dimension. DTT was added in a 1 mM concentration. Intensities of isolated correlation peaks that were previously assigned (*23*, *24*) were compared between identical spectra recorded on ^{15}N-labeled Tau samples with or without paclitaxel-stabilized MTs.

Fluorescence Assay. Acrylodan labeling of Tau and purification were performed as described (*19*). To avoid problems with absorption of the residual fluorophore, ^{15}N-labeled Tau was used for this fluorophore labeling, allowing accurate determination of its concentration by comparison of its signal intensity in a 1D $^{1}H-^{15}N$ HSQC spectrum with that of an absorption dosed ^{15}N-labeled sample before acrylodan labeling. The fluorescence assay was performed by titrating increasing concentrations of acrylodan-labeled Tau into a 1 μM paclitaxel-stabilized MT solution. Spectra were acquired on a PTI fluorimeter at 20 °C. We monitored the fluorescence signal from 460 to 540 nm after excitation at 290 nm. Data correction and fitting of the data were identical as in ref *19*. Briefly, the equation $F = F_{max}(b - (b^2 - 4ac)^{0.5})/2a + y$ was fitted to the data, where F is the experimental fluorescence emission intensity at 490 nm for a given acrylodan-Tau concentration c, F_{max} is the fluorescence at saturating Tau levels, a is the concentration of Tau binding sites, $b = a + c + K_D$, and y is the y-intercept value. The maximal stoichiometry of binding, n, was derived from $a = n \times$ tubulin concentration.

ACKNOWLEDGMENT

We thank Drs. M. Knossow and B. Gigant (Gif-sur-Yvette, France) for careful reading of the manuscript and useful suggestions.

SUPPORTING INFORMATION AVAILABLE

Plots of the residual intensity of the Tau-[163−441] fragment and of Tau without DTT and PKA phosphorylated when bound to paclitaxel-stabilized microtubules. This material is available free of charge via the Internet at http://pubs.acs.org.

REFERENCES

1. Buee, L., Bussiere, T., Buee-Scherrer, V., Delacourte, A., and Hof, P. R. (2000) Tau protein isoforms, phosphorylation and role in neurodegenerative disorders, *Brain Res. Brain Res. Rev. 33*, 95−130.
2. Nogales, E., Wolf, S. G., and Downing, K. H. (1998) Structure of the alpha/beta tubulin dimer by electron crystallography, *Nature 391*, 199−203.
3. Nogales, E., Whittaker, M., Milligan, R. A., and Downing, K. H. (1999) High-resolution model of the microtubule, *Cell 96*, 79−88.
4. Cleveland, D. W., Hwo, S. Y., and Kirschner, M. W. (1977) Physical and chemical properties of purified Tau factor and the role of Tau in microtubule assembly, *J. Mol. Biol. 116*, 227−47.
5. Schweers, O., Schonbrunn-Hanebeck, E., Marx, A., and Mandelkow, E. (1994) Structural studies of Tau protein and Alzheimer paired helical filaments show no evidence for beta-structure, *J. Biol. Chem. 269*, 24290−7.
6. Goode, B. L., Denis, P. E., Panda, D., Radeke, M. J., Miller, H. P., Wilson, L., and Feinstein, S. C. Functional interactions between the proline-rich and repeat regions of Tau enhance microtubule binding and assembly, (1997) *Mol. Biol. Cell 8*, 353−365.
7. Barre, P., and Eliezer, D. Folding of the Repeat Domain of Tau Upon Binding to Lipid Surfaces, (2006) *J. Mol. Biol. 362*, 312−326.
8. Chau, M. F., Radeke, M. J., de Ines, C., Barasoain, I., Kohlstaedt, L. A., and Feinstein, S. C. (1998) The microtubule-associated protein Tau cross-links to two distinct sites on each alpha and beta tubulin monomer via separate domains, *Biochemistry 37*, 17692−703.
9. Delacourte, A., and Defossez, A. (1986) Alzheimer's disease: Tau proteins, the promoting factors of microtubule assembly, are major components of paired helical filaments, *J. Neurol. Sci. 76*, 173−86.
10. Grundke-Iqbal, I., Iqbal, K., Quinlan, M., Tung, Y. C., Zaidi, M. S., and Wisniewski, H. M. (1986) Microtubule-associated protein Tau. A component of Alzheimer paired helical filaments, *J. Biol. Chem. 261*, 6084−9.
11. Rissman, R. A., Poon, W. W., Blurton-Jones, M., Oddo, S., Torp, R., Vitek, M. P., LaFerla, F. M., Rohn, T. T., and Cotman, C. W. (2004) Caspase-cleavage of Tau is an early event in Alzheimer disease tangle pathology, *J. Clin. Invest. 114*, 121−30.

12. Lindwall, G., and Cole, R. D. (1984) Phosphorylation affects the ability of Tau protein to promote microtubule assembly, *J. Biol. Chem. 259*, 5301−5.
13. Biernat, J., Gustke, N., Drewes, G., Mandelkow, E. M., and Mandelkow, E. (1993) Phosphorylation of Ser262 strongly reduces binding of Tau to microtubules: distinction between PHF-like immunoreactivity and microtubule binding, *Neuron 11*, 153−63.
14. Mandelkow, E. M., Biernat, J., Drewes, G., Gustke, N., Trinczek, B., and Mandelkow, E. (1995) Tau domains, phosphorylation, and interactions with microtubules, *Neurobiol. Aging 16*, 355−62.
15. Hasegawa, M., Morishima-Kawashima, M., Takio, K., Suzuki, M., Titani, K., and Ihara, Y. (1992) Protein sequence and mass spectrometric analyses of Tau in the Alzheimer's disease brain, *J. Biol. Chem. 267*, 17047−54.
16. Gustke, N., Trinczek, B., Biernat, J., Mandelkow, E. M., and Mandelkow, E. (1994) Domains of Tau protein and interactions with microtubules, *Biochemistry 33*, 9511−22.
17. Santarella, R. A., Skiniotis, G., Goldie, K. N., Tittmann, P., Gross, H., Mandelkow, E. M., Mandelkow, and E., Hoenger, A. (2004) Surface-decoration of microtubules by human Tau, *J. Mol. Biol. 339*, 539−53.
18. Scott, C. W., Klika, A. B., Lo, M. M., Norris, T. E., and Caputo, C. B. (1992) Tau protein induces bundling of microtubules in vitro: comparison of different Tau isoforms and a Tau protein fragment, *J. Neurosci. Res. 33*, 19−29.
19. Makrides, V., Massie, M. R., Feinstein, S. C., and Lew, J. (2004) Evidence for two distinct binding sites for Tau on microtubules, *Proc. Natl. Acad. Sci. U.S.A. 101*, 6746−51.
20. Ackmann, M., Wiech, H., and Mandelkow, E. (2000) Nonsaturable binding indicates clustering of Tau on the microtubule surface in a paired helical filament-like conformation, *J. Biol. Chem. 275*, 30335−43.
21. Hitt, A. L., Cross, A. R., and Williams, R. C., Jr. (1990) Microtubule solutions display nematic liquid crystalline structure, *J. Biol. Chem. 265*, 1639−47.
22. Mukrasch, M. D., Biernat, J.; von Bergen, M., Griesinger, C., Mandelkow, E., and Zweckstetter, M. (2005) Sites of Tau important for aggregation populate {beta}-structure and bind to microtubules and polyanions, *J. Biol. Chem. 280*, 24978−86.
23. Lippens, G., Wieruszeski, J. M., Leroy, A., Smet, C., Sillen, A., Buee, L., and Landrieu, I. (2004) Proline-directed random-coil chemical shift values as a tool for the NMR assignment of the Tau phosphorylation sites, *ChemBioChem 5*, 73−8.
24. Smet, C., Leroy, A., Sillen, A., Wieruszeski, J. M., Landrieu, I., and Lippens, G. (2004) Accepting its random coil nature allows a partial NMR assignment of the neuronal Tau protein, *ChemBioChem 5*, 1639−46.
25. Eliezer, D., Barre, P., Kobaslija, M., Chan, D., Li, X., and Heend, L. (2005) Residual structure in the repeat domain of Tau: echoes of microtubule binding and paired helical filament formation, *Biochemistry 44*, 1026−36.
26. Landino, L. M., Skreslet, T. E., and Alston, J. A. (2004) Cysteine oxidation of Tau and microtubule-associated protein-2 by peroxynitrite: modulation of microtubule assembly kinetics by the thioredoxin reductase system, *J. Biol. Chem. 279*, 35101−5.
27. Zheng-Fischhofer, Q., Biernat, J., Mandelkow, E. M., Illenberger, S., Godemann, R., and Mandelkow, E. (1998) Sequential phosphorylation of Tau by glycogen synthase kinase-3beta and protein kinase A at Thr212 and Ser214 generates the Alzheimer-specific epitope of antibody AT100 and requires a paired-helical-filament-like conformation, *Eur. J. Biochem. 252*, 542−52.
28. Landrieu, I., Lacosse, L., Leroy, A., Wieruszeski, J. M., Trivelli, X., Sillen, A., Sibille, N., Schwalbe, H., Saxena, K., Langer, T., and Lippens, G. (2006) NMR analysis of a Tau phosphorylation pattern, *J. Am. Chem. Soc. 128*, 3575−83.
29. Butner, D. A., and Kirschner, M. W. (1991) Tau protein binds to microtubules through a flexible array of distributed weak sites, *J. Cell Biol. 115*, 717−30.
30. Woody, R. W., Roberts, G. C., Clark, D. C., and Bayley, P. M. (1982) 1H NMR evidence for flexibility in microtubule-associated proteins and microtubule protein oligomers, *FEBS Lett. 141*, 181−4.
31. Pervushin, K., Riek, R., Wider, G., and Wuthrich, K. (1997) Attenuated T2 relaxation by mutual cancellation of dipole-dipole coupling and chemical shift anisotropy indicates an avenue to NMR structures of very large biological macromolecules in solution, *Proc. Natl. Acad. Sci. U.S.A. 94* (23, Nov 11), 12366−71.
32. Chen, J., Kanai, Y., Cowan, N. J., and Hirokawa, N. (1992) Projection domains of MAP2 and tau determine spacings between microtubules in dendrites and axons, *Nature 260*, 674−6.
33. Frappier, T. F., Georgieff, I. S., Brown, K., and Shelanski, M. L. (1994) Tau Regulation of microtubule-microtubule spacing and bundling, *J. Neurochem. 63*, 2288−94.
34. Ross, J. L., Santangelo, C. D., Makrides, V., and Fygenson, D. K. (2005) Tau induces cooperative Taxol binding to microtubules, *Proc. Natl. Acad. Sci. U.S.A. 101*, 12910−5.
35. Sillen, A., Leroy, A., Wieruszeski, J. M., Loyens, A., Beauvillain, J. C., Buee, L., Landrieu, I., and Lippens, G. (2005) Regions of Tau implicated in the paired helical fragment core as defined by NMR, *ChemBioChem 6*, 1849−56.
36. Redeker, V., Melki, R., Prome, D., Le Caer, J. P., and Rossier, J. (1992) Structure of tubulin C-terminal domain obtained by subtilisin treatment. The major alpha and beta tubulin isotypes from pig brain are glutamylated, *FEBS Lett. 313*, 185−92.
37. Serrano, L., Avila, J., and Maccioni, R. B. (1984) Controlled proteolysis of tubulin by subtilisin: localization of the site for MAP2 interaction, *Biochemistry 23*, 4675−81.
38. Littauer, U. Z., Giveon, D., Thierauf, M., Ginzburg, I., and Ponstingl, H. (1986) Common and distinct tubulin binding sites for microtubule-associated proteins, *Proc. Natl. Acad. Sci. U.S.A. 83*, 7162−6.
39. Lee, G., Cowan, N., and Kirschner, M. (1988) The primary structure and heterogeneity of tau protein from mouse brain, *Science 239*, 285−8.
40. Himmler, A., Drechsel, D., Kirschner, M., and Martin, D. (1989) Tau consists of a set of proteins with repeated C-terminal microtubule-binding domains and variable N-terminal domains, *Mol. Cell. Biol. 9*, 1381−8.
41. Goode, B. L., and Feinstein, S. C. (1994) Identification of a novel microtubule binding and assembly domain in the developmentally regulated inter-repeat region of Tau, *J. Cell Biol. 124*, 769−82.
42. Scott, C. W., Spreen, R. C., Herman, J. L., Chow, F. P., Davison, M. D., Young, J., and Caputo, C. B. (1993) Phosphorylation of recombinant tau by cAMP-dependent protein kinase. Identification of phosphorylation sites and effect on microtubule assembly, *J. Biol. Chem. 268*, 1166−73.
43. Schneider, A., Biernat, J., von Bergen, M., Mandelkow, E., and Mandelkow, E. M. (1999) Phosphorylation that detaches tau protein from microtubules (Ser262, Ser214) also protects it against aggregation into Alzheimer paired helical filaments, *Biochemistry 38*, 3549−58.
44. Lin, M. T., and Beal, M. F. (2006) Mitochondrial dysfunction and oxidative stress in neurodegenerative diseases, *Nature 443*, 787−95.
45. Lewis, S. A., Ivanov, I. E., Lee, G. H., and Cowan, N. J. (1989) Organization of microtubules in dendrites and axons is determined by a short hydrophobic zipper in microtubule-associated proteins MAP2 and tau, *Nature 342*, 498−505.
46. Al-Bassam, J., Ozer, R. S., Safer, D., Halpain, S., and Milligan, R. A. (2002) MAP2 and tau bind longitudinally along the outer ridges of microtubule protofilaments, *J. Cell Biol. 157*, 1187−96.
47. Kar, S., Fan, J., Smith, M. J., Goedert, M., and Amos, L. A. (2003) Repeat motifs of Tau bind to the insides of microtubules in the absence of taxol, *EMBO J. 22*, 70−7.
48. Devred, F., Barbier, P., Douillard, S., Monasterio, O., Andreu, J. M., and Peyrot, V. (2004) Tau induces ring and microtubule formation from alphabeta-tubulin dimers under nonassembly conditions, *Biochemistry 43*, 10520−31.
49. Fiaux, J., Bertelsen, E. B., Horwich, A. L., and Wüthrich, K. (2002) NMR analysis of a 900K GroEL GroES complex, *Nature 418*, 207−11.
50. Barbier, P., Peyrot, V., Leynadier, D., and Andreu, J. M. (1998) The active GTP- and ground GDP-liganded states of tubulin are distinguished by the binding of chiral isomers of ethyl 5-amino-2-methyl-1,2-dihydro-3-phenylpyrido[3,4-b]pyrazin-7-yl carbamate, *Biochemistry 37*, 758−68.
51. Ellman, G. L. (1959) Tissue sulfhydryl groups, *Arch. Biochem. Biophys. 82*, 70−7.

BI061920I